COMMISSIONS G1 AND G4 OF THE IAU
INFORMATION BULLETIN ON VARIABLE STARS
Volume 62 Number 6190 DOI: 10.22444/IBVS.6190

Konkoly Observatory
Budapest
15 December 2016

*HU ISSN 0374 – 0676*

# NEW R CORONAE BOREALIS AND DY PERSEI CANDIDATES IN THE SMC

NIKZAT, F.[1,2]; CATELAN, M.[1,2]

[1] Instituto de Astrofísica, Facultad de Física, Pontificia Universidad Católica de Chile, Av. Vicuña Mackenna 4860, 782-0436 Macul, Santiago, Chile; e-mail: fnikzat@astro.puc.cl, mcatelan@astro.puc.cl

[2] Millennium Institute of Astrophysics, Santiago, Chile

R Coronae Borealis (RCB) stars are C-rich, H-deficient red supergiants that undergo dramatic dimming episodes at irregular intervals. The dimming episodes are caused by self-obscuration by dust, occurring as a consequence of mass loss events (e.g., Lambert & Rao 1994; Clayton 1996, 2012; Catelan & Smith 2015, and references therein). The purpose of this contribution is to report on a new search for RCB stars in the Small Magellanic Cloud (SMC), carried out using $VI$ light curves from the OGLE project (Soszyński et al. 2011). To detect candidates, the $VI$ light curves of all SMC red variable stars were visually inspected, and compared against templates from the literature. New RCB candidates were detected in the process, which had previously been classified as semi-regular or Mira variables. Additionally, DY Persei candidates were also identified. Compared to their RCB counterparts, the DY Per stars tend to be cooler, have slower decline rates, and more symmetrical declines (e.g., Začs et al. 2007; Catelan & Smith 2015, and references therein). If confirmed, these detections would lead to a significant increase in the number of known RCB + DY Per stars in the SMC.

The RCB stars have traditionally been classified as eruptive variables, due to their massive ejection episodes. However, they may also be classified as *self-eclipsing variable stars*, because of the self-obscuration due to formation of carbon dust around the star during mass loss events. Consequently, the RCB stars show a deep drop in their light curves which is a distinguishing characteristic of this class of variables. Since the dust forms in discrete clouds, the declines only occur when dust condenses along our line of sight.

The evolutionary origin of the RCB stars is not understood yet. Two scenarios have been proposed for their formation (Iben et al. 1996; Saio & Jeffery 2002): a merger of two white dwarfs or a final He-shell flash of the central object of a planetary nebula-hosting post-asymptotic giant branch (AGB) star. In the latter case, they would represent so-called "born-again stars," to the extent that they would constitute (pre-) white dwarf stars that have been brought back to giant dimensions (Renzini 1990); in the former, they would be low-mass analogs of the same process that is believed to result in type Ia supernovae.

RCB stars are rare, with only about a hundred currently known (Tisserand et al. 2016), of which roughly one quarter are found in the Magellanic Clouds (Tisserand et al. 2013). To properly understand their evolutionary origin, more RCB stars in different

environments with different metallicities are required. Furthermore, AGB stars are known as one of the main producers of dust to the interstellar medium (ISM), and likewise RCB stars may also significantly contribute to the dust enrichment of the ISM. As dust has different behavior in different environments, building significant samples of low-metallicity RCB stars can provide useful constraints on the role such stars may have played in the course of cosmic history.

In this note, we present new RCB candidates found in the relatively low-metallicity environment of the SMC, based on an analysis of the morphology of the light curves of red variables published by the OGLE team. Their names and coordinates are provided in Table 1. To date, only three RCB and three DY Per stars have been confirmed in the SMC (Tisserand et al. 2009), with an additional two RCB plus three DY Per candidates also having been reported in the literature (Kraemer et al. 2005; Tisserand et al. 2009). Most recently, a new RCB candidate, Gaia16aau, was discovered using Gaia data (Tisserand et al. 2016).

The catalog data for red variable stars in the SMC are available online from the OGLE project.[1] The data were taken with the 1.3-meter Warsaw telescope at Las Campanas Observatory, northern Chile, in the course of the OGLE-III campaigns (Soszyński et al. 2011). All $VI$ light curves were visually inspected, in a search for dramatic, non-periodic drops in brightness that might be indicative of RCB-like behavior. Our results are summarized in Table 1 and Figures 1 through 14. In total, we present two new RCB (Fig. 1) and 63 new DY Per (Figs. 2-14) candidates. A third RCB candidate was also identified, and will be discussed later in this note.

For completeness, previously confirmed and candidate RCB and DY Per stars in the SMC are also listed in Table 2. Among these, three confirmed DY Per stars (OGLE-SMC-LPV-03068, OGLE-SMC-LPV-04633, OGLE-SMC-LPV-11903) and three DY Per candidates (OGLE-SMC-LPV-05023, OGLE-SMC-LPV-06616, OGLE-SMC-LPV-12291) from the EROS2 project (Tisserand et al. 2009) were detected in the OGLE data. Their corresponding light curves are shown in Figures 15 and 16 for the confirmed and candidate DY Per stars, respectively. Note that we include OGLE-SMC-LPV-05007 among the DY Per candidates in this paper, even though it was rejected by Tisserand et al. (2009) due to the presence of strong TiO bands. However, the light curve morphology bears some resemblance to those of other C-rich stars, and indeed the star has been classified as a C-star in the OGLE-III catalog. This star may thus be an interesting example of what might perhaps be called a "borderline" DY Per-like star, not clearly conforming to the canonical DY Per classification scheme. Its coordinates are given in the bottom row of Table 2.

We emphasize, in this context, that OGLE-SMC-LPV-11903[2] (EROS2-SMC-DYPer-3), which has previously been classified as a DY Per star based on spectroscopic data, presents a light curve morphology that is strongly reminiscent of an RCB star (Fig. 15). This may also hint at the possibility of a "transitional" DY Per/RCB status. The latter might be consistent with the presence of an evolutionary sequence among hydrogen-deficient carbon stars, as suggested by Saio & Jeffery (2002) and supported by De Marco et al. (2002) and Schaefer (2016).

We also note that, while OGLE-SMC-LPV-03068 (EROS2-SMC-DYPer-2) is classified as an O-type LPV in the OGLE-III catalog, it has already been spectroscopically confirmed to be a DY Per C-star (see Tisserand et al. 2004, 2009). The star's light curve, as shown in Figure 15, is indeed consistent with that expected for a C-star.

[1] `ftp://ftp.astrouw.edu.pl/ogle/ogle3/OIII-CVS/smc/lpv/`

[2] Note that the OGLE-2 ID for this star is missing in the OGLE-III catalog.

We were able to match the spectroscopic RCB candidate MSX-SMC-014 (Kraemer et al. 2005; Tisserand et al. 2009) to OGLE-SMC-LPV-05719; the light curve is shown in Figure 17. We point out that this light curve bears some resemblance to that of OGLE-SMC-LPV-17611; in both cases, we see several photometric declines during the OGLE-III monitoring, and the time interval between adjacent minima/maxima is roughly similar (Fig. 17). We accordingly propose OGLE-SMC-LPV-17611 as an additional candidate RCB star in the SMC.

To close, we note that, in our work, we have only used light curve morphology as indicative of potential RCB/DY Per status. Follow-up observations, both photometric and spectroscopic, are required in order to conclusively establish the nature of our candidates.

**Acknowledgments**: We warmly thank the referee, E. J. Montiel, for his thoughtful report. Support for this project is provided by the Ministry for the Economy, Development, and Tourism's Millennium Science Initiative through grant IC 120009, awarded to the Millennium Institute of Astrophysics (MAS); by Proyecto Basal PFB-06/2007; by CONICYT's PCI program through grant DPI20140066; and by FONDECYT grants #1141141. FN is grateful for financial support by Proyecto Gemini CONICYT grants #32130013 and #32140036.

References:

Catelan, M., Smith, H. A., 2015, *Pulsating Stars* (Wiley-VCH)
Clayton, G. C., 1996, *PASP*, **108**, 225 DOI
Clayton, G. C., 2012, *JAAVSO*, **40**, 539
De Marco, O., Clayton, G. C., Herwig, F., et al., 2002, *AJ*, **123**, 3387 DOI
Iben, I., Tutukov, A. V., Yungelson, L. R., 1996, *ApJ*, **456**, 750 DOI
Kraemer, K. E., Sloan, G. C., Wood, P. R., et al., 2005, *ApJ*, **631**, L147 DOI
Lambert, D. L., & Rao, N. K., 1994, *JApA*, **15**, 47 DOI
Renzini, A., 1990, *ASPC*, **11**, 549
Saio, H., & Jeffery, C. S., 2002, *MNRAS*, **333**, 121 DOI
Schaefer, B. E., 2016, *MNRAS*, **460**, 1233 DOI
Soszyński, I., Udalski, A., Szymański, M. K., et al., 2011, *AcA*, **61**, 217
Tisserand, P., Clayton, G. C., Welch, D. L., et al., 2013, *A&A*, **551**, A77 DOI
Tisserand, P., Marquette, J. B., Beaulieu, J. P., et al., 2004, *A&A*, **424**, 245 DOI
Tisserand, P., Wood, P. R., Marquette, J. B., et al., 2009, *A&A*, **501**, 985 DOI
Tisserand, P., Wyrzykowski, L., Clayton, G., et al., 2016, *ATel*, **8681**, 1
Začs, L., Mondal, S., Chen, W. P., et al., 2007, *A&A*, **472**, 247 DOI

Table 1: New RCB and DY Per candidates in the SMC

| | | | | |
|---|---|---|---|---|
| New RCB candidates (*this note*) | | | | |
| OGLE-SMC-LPV-01019 | 00:31:16.77 | −73:56:48.6 | | SRV |
| OGLE-SMC-LPV-06216 | 00:47:05.33 | −72:34:30.5 | MACHO-208.15801.1 | SRV |
| OGLE-SMC-LPV-17611 | 01:09:21.69 | −71:24:35.1 | | Mira |
| New DY Per candidates (*this note*) | | | | |
| OGLE-SMC-LPV-00190 | 00:23:58.50 | −73:37:54.9 | | Mira |
| OGLE-SMC-LPV-00486 | 00:27:10.92 | −73:24:30.3 | | Mira |
| OGLE-SMC-LPV-00492 | 00:27:14.50 | −73:36:42.4 | | Mira |
| OGLE-SMC-LPV-00666 | 00:28:34.78 | −74:05:41.9 | | SRV |
| OGLE-SMC-LPV-00799 | 00:29:42.22 | −73:19:11.1 | | SRV |
| OGLE-SMC-LPV-02715 | 00:39:13.28 | −73:57:05.9 | | SRV |
| OGLE-SMC-LPV-03078 | 00:40:16.26 | −73:01:15.5 | | Mira |
| OGLE-SMC-LPV-03315 | 00:40:55.61 | −72:47:49.4 | | Mira |
| OGLE-SMC-LPV-03429 | 00:41:16.95 | −72:52:16.8 | MACHO-213.15398.77 | Mira |
| OGLE-SMC-LPV-03593 | 00:41:42.45 | −72:58:53.7 | MACHO-213.15453.892 | Mira |
| OGLE-SMC-LPV-03810 | 00:42:16.10 | −72:57:32.6 | | SRV |
| OGLE-SMC-LPV-04208 | 00:43:09.58 | −73:09:20.1 | | Mira |
| OGLE-SMC-LPV-04575 | 00:43:56.94 | −73:56:08.0 | | Mira |
| OGLE-SMC-LPV-05322 | 00:45:33.00 | −73:05:12.1 | MACHO-212.15679.930 | Mira |
| OGLE-SMC-LPV-05801 | 00:46:23.52 | −72:37:39.8 | | Mira |
| OGLE-SMC-LPV-06089 | 00:46:50.78 | −71:47:39.4 | | SRV |
| OGLE-SMC-LPV-06156 | 00:46:59.11 | −73:25:18.8 | MACHO-212.15788.31 | SRV |
| OGLE-SMC-LPV-06572 | 00:47:37.82 | −73:00:13.3 | MACHO-212.15795.25 | SRV |
| OGLE-SMC-LPV-06962 | 00:48:12.30 | −72:41:18.6 | | SRV |
| OGLE-SMC-LPV-07113 | 00:48:27.01 | −72:45:55.5 | MACHO-208.15855.5029 | Mira |
| OGLE-SMC-LPV-07354 | 00:48:50.92 | −73:14:02.3 | | SRV |
| OGLE-SMC-LPV-07375 | 00:48:52.49 | −73:08:56.8 | MACHO-212.15907.28 | Mira |
| OGLE-SMC-LPV-07665 | 00:49:20.53 | −72:34:11.8 | MACHO-208.15915.2828 | Mira |
| OGLE-SMC-LPV-07829 | 00:49:34.97 | −73:18:18.5 | MACHO-212.15904.2217 | SRV |
| OGLE-SMC-LPV-08192 | 00:50:12.59 | −72:33:42.3 | MACHO-208.15972.2547 | SRV |
| OGLE-SMC-LPV-08390 | 00:50:31.29 | −72:29:13.1 | MACHO-208.15973.50 | Mira |
| OGLE-SMC-LPV-08445 | 00:50:37.00 | −73:08:53.7 | | SRV |
| OGLE-SMC-LPV-08741 | 00:51:04.65 | −72:01:37.6 | | SRV |
| OGLE-SMC-LPV-08803 | 00:51:10.37 | −72:27:42.8 | | Mira |
| OGLE-SMC-LPV-08931 | 00:51:23.06 | −72:36:16.4 | | SRV |
| OGLE-SMC-LPV-09350 | 00:51:58.14 | −73:43:35.3 | | SRV |
| OGLE-SMC-LPV-09801 | 00:52:40.18 | −72:47:27.7 | MACHO-207.16140.490 | Mira |
| OGLE-SMC-LPV-10280 | 00:53:23.12 | −72:04:22.4 | | SRV |
| OGLE-SMC-LPV-10436 | 00:53:37.31 | −72:34:35.2 | MACHO-207.16200.324 | Mira |
| OGLE-SMC-LPV-10465 | 00:53:40.01 | −72:52:18.7 | | SRV |
| OGLE-SMC-LPV-10816 | 00:54:10.75 | −73:03:03.1 | MACHO-211.16250.24 | SRV |
| OGLE-SMC-LPV-11279 | 00:54:54.11 | −73:03:18.2 | MACHO-211.16250.4090 | Mira |
| OGLE-SMC-LPV-11698 | 00:55:34.14 | −72:40:29.4 | MACHO-207.16313.24 | SRV |
| OGLE-SMC-LPV-11806 | 00:55:44.47 | −72:54:40.8 | | Mira |
| OGLE-SMC-LPV-12043 | 00:56:10.05 | −72:28:41.9 | | Mira |
| OGLE-SMC-LPV-12119 | 00:56:16.38 | −72:16:41.4 | MACHO-207.16376.687 | Mira |
| OGLE-SMC-LPV-12304 | 00:56:36.77 | −73:32:55.5 | | SRV |
| OGLE-SMC-LPV-12427 | 00:56:50.29 | −72:25:08.7 | MACHO-207.16373.675 | Mira |
| OGLE-SMC-LPV-13205 | 00:58:20.78 | −72:55:02.1 | MACHO-211.16480.1110 | SRV |
| OGLE-SMC-LPV-13251 | 00:58:26.59 | −73:40:35.0 | | SRV |
| OGLE-SMC-LPV-13320 | 00:58:34.86 | −73:32:10.9 | | SRV |
| OGLE-SMC-LPV-13323 | 00:58:35.18 | −72:59:35.6 | MACHO-211.16479.2 | SRV |
| OGLE-SMC-LPV-13676 | 00:59:15.78 | −72:27:54.6 | MACHO-207.16544.36 | Mira |
| OGLE-SMC-LPV-13739 | 00:59:21.90 | −72:11:13.4 | | SRV |
| OGLE-SMC-LPV-13749 | 00:59:23.36 | −73:56:01.0 | | SRV |
| OGLE-SMC-LPV-14197 | 01:00:15.67 | −72:22:26.2 | MACHO-207.16602.106 | SRV |
| OGLE-SMC-LPV-14205 | 01:00:16.84 | −72:55:18.1 | | Mira |
| OGLE-SMC-LPV-14322 | 01:00:31.66 | −72:14:49.1 | MACHO-207.16604.926 | Mira |
| OGLE-SMC-LPV-14778 | 01:01:26.59 | −72:47:41.2 | | Mira |
| OGLE-SMC-LPV-14991 | 01:01:54.59 | −72:58:22.4 | MACHO-211.16707.28 | Mira |
| OGLE-SMC-LPV-16113 | 01:04:39.84 | −72:49:48.2 | | Mira |

Table 1: cont.

| Star name | Ra (J2000) | DEC (J2000) | Other ID | Subtype |
|---|---|---|---|---|
| OGLE-SMC-LPV-16844 | 01:06:53.07 | −73:46:00.2 | | Mira |
| OGLE-SMC-LPV-16850 | 01:06:54.81 | −72:24:41.2 | | Mira |
| OGLE-SMC-LPV-17194 | 01:08:01.14 | −72:53:17.4 | | SRV |
| OGLE-SMC-LPV-17267 | 01:08:12.97 | −72:52:44.0 | | Mira |
| OGLE-SMC-LPV-17976 | 01:10:53.22 | −72:14:46.0 | | SRV |
| OGLE-SMC-LPV-18657 | 01:15:09.88 | −72:05:51.3 | | Mira |
| OGLE-SMC-LPV-19032 | 01:18:48.06 | −72:27:43.7 | | Mira |

Table 2: Known RCB and DY Per stars in the SMC

| Star name | RA (J2000) | DEC (J2000) | Other ID |
|---|---|---|---|
| RCB and DY Per confirmed | | | |
| EROS2-SMC-RCB-1 | 00:37:47.11 | −73:39:02.3 | RAW-21 |
| EROS2-SMC-RCB-2 | 00:48:22.96 | −73:41:04.7 | RAW-476 |
| EROS2-SMC-RCB-3 | 00:57:18.15 | −72:42:35.2 | MACHO-207.16426.1662 |
| EROS2-SMC-DYPer-1 | 00:44:07.50 | −72:44:16.4 | RAW-233 |
| | | | MACHO-208.15571.60 |
| | | | OGLE-SMC-LPV-04633 |
| EROS2-SMC-DYPer-2 | 00:40:14.72 | −74:11:21.6 | [MH95]-431 |
| | | | OGLE-SMC-LPV-03068 |
| EROS2-SMC-DYPer-3 | 00:55:54.97 | −72:35:12.27 | RAW-961 |
| | | | OGLE2-SMC-SC7-368043 |
| | | | OGLE-SMC-LPV-11903 |
| RCB and DY Per candidates | | | |
| EROS2-SMC-RCB-4 | 01:04:52.89 | −72:04:02.64 | OGLE2-SMC-SC10-107856 |
| MSX-SMC-014 | 00:46:16.33 | −74:11:13.6 | OGLE-SMC-LPV-05719 |
| Gaia16aau | 00:50:10.67 | −69:43:57.9 | [MH95]-580 |
| | | | OGLE-SMC710.08.1 |
| EROS2-SMC-DYPer-4 | 00:56:35.47 | −71:32:32.66 | [MH95]-672 |
| | | | OGLE-SMC-LPV-12291 |
| EROS2-SMC-DYPer-5 | 00:47:41.71 | −73:06:16.38 | RAW-421 |
| | | | MACHO-212.15793.25 |
| | | | OGLE-SMC-LPV-06616 |
| EROS2-SMC-DYPer-6 | 00:44:56.40 | −73:12:25.02 | MACHO-212.15621.153 |
| | | | OGLE-SMC-LPV-05023 |
| "Borderline" DY Per-like candidate (*see text*) | | | |
| sm0101n-16084 | 00:44:54.02 | −73:15:30.02 | MACHO-212.15620.713 |
| | | | OGLE-SMC-LPV-05007 |

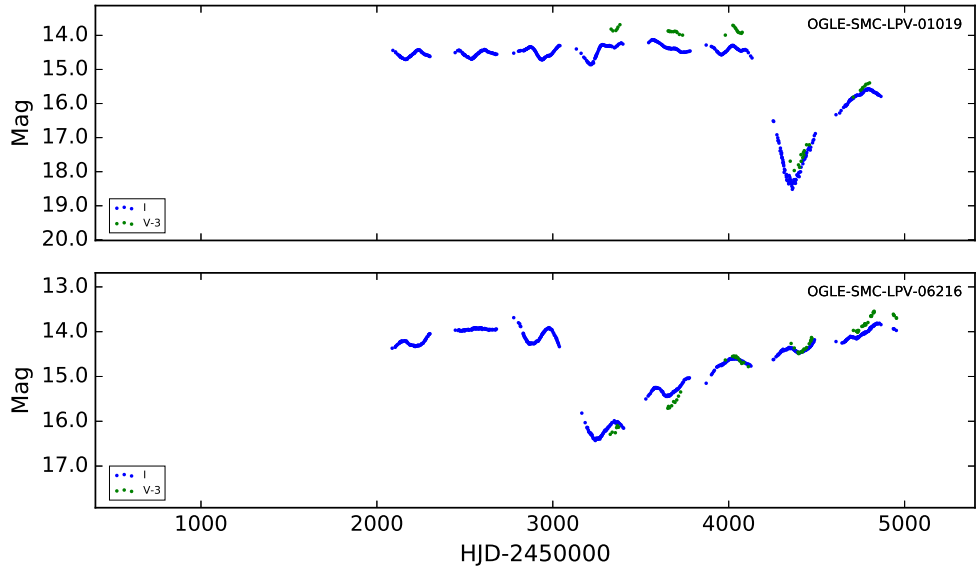


**Figure 1.** Light curves in $I$ (*blue*) and $V$ (*green*) of two new RCB candidates in the SMC.

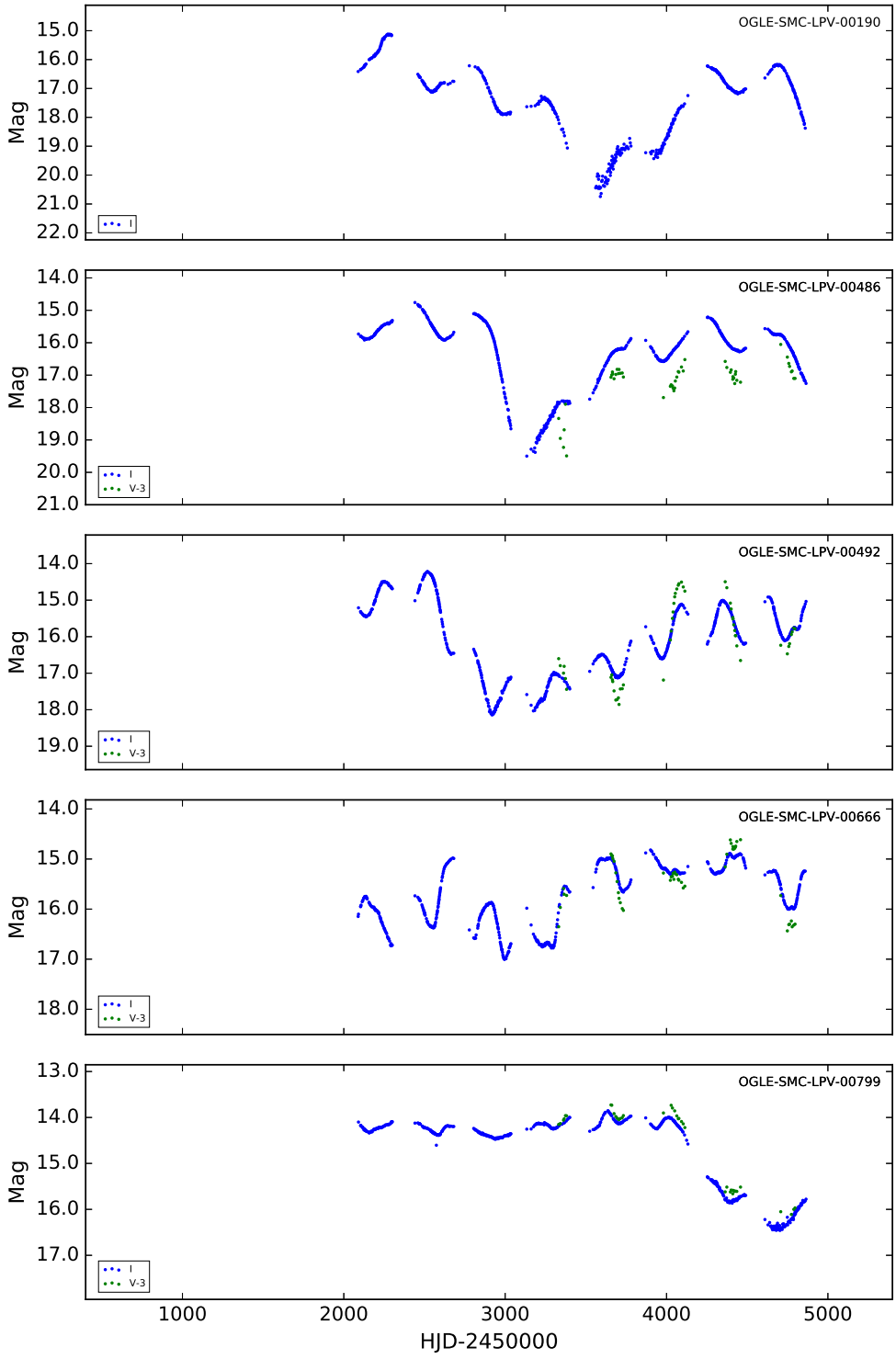


**Figure 2.** Light curves in $I$ (*blue*) and $V$ (*green*) of new DY Per candidates in the SMC.

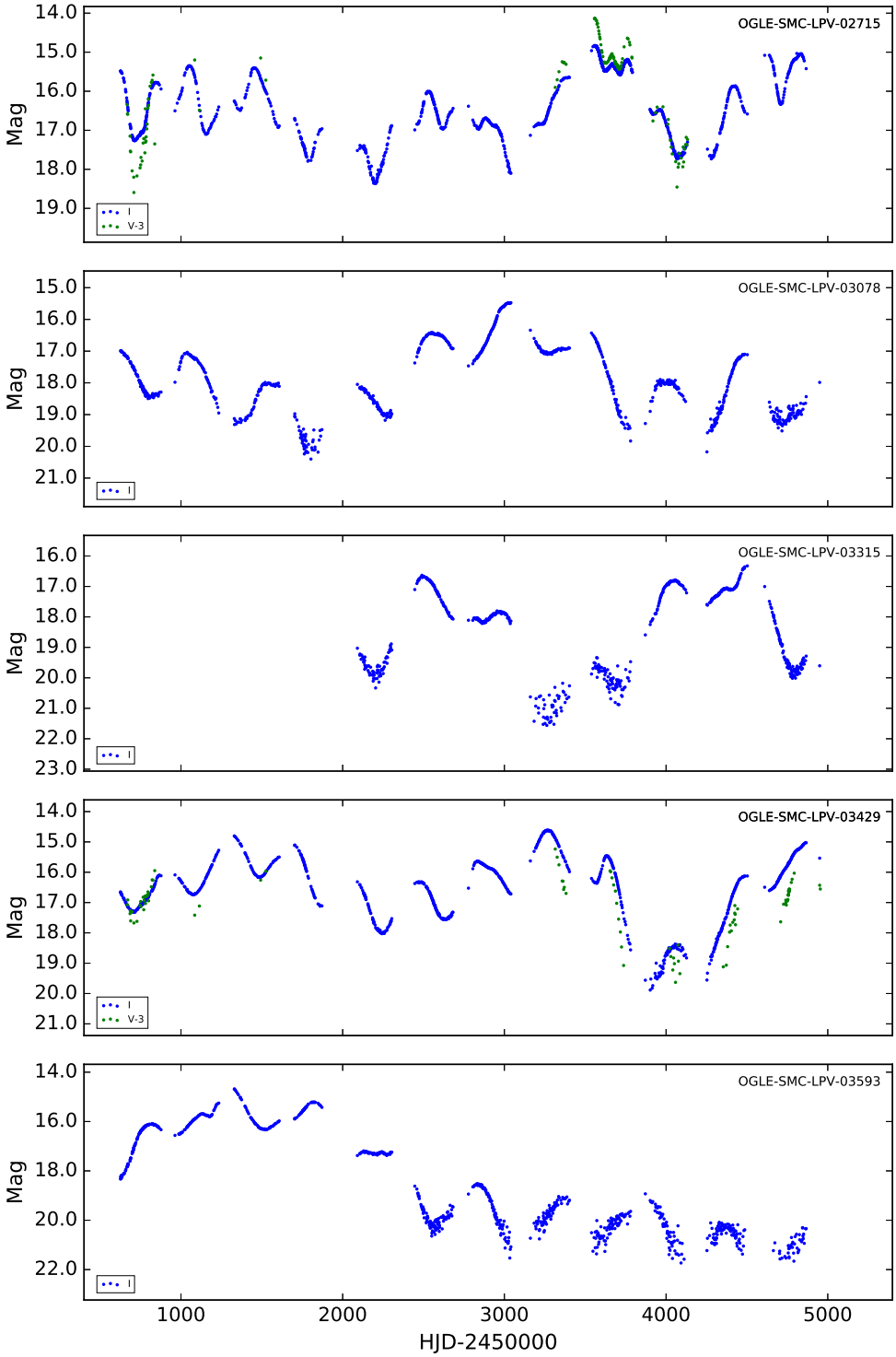


**Figure 3.** Light curves in $I$ (*blue*) and $V$ (*green*) of new DY Per candidates in the SMC.

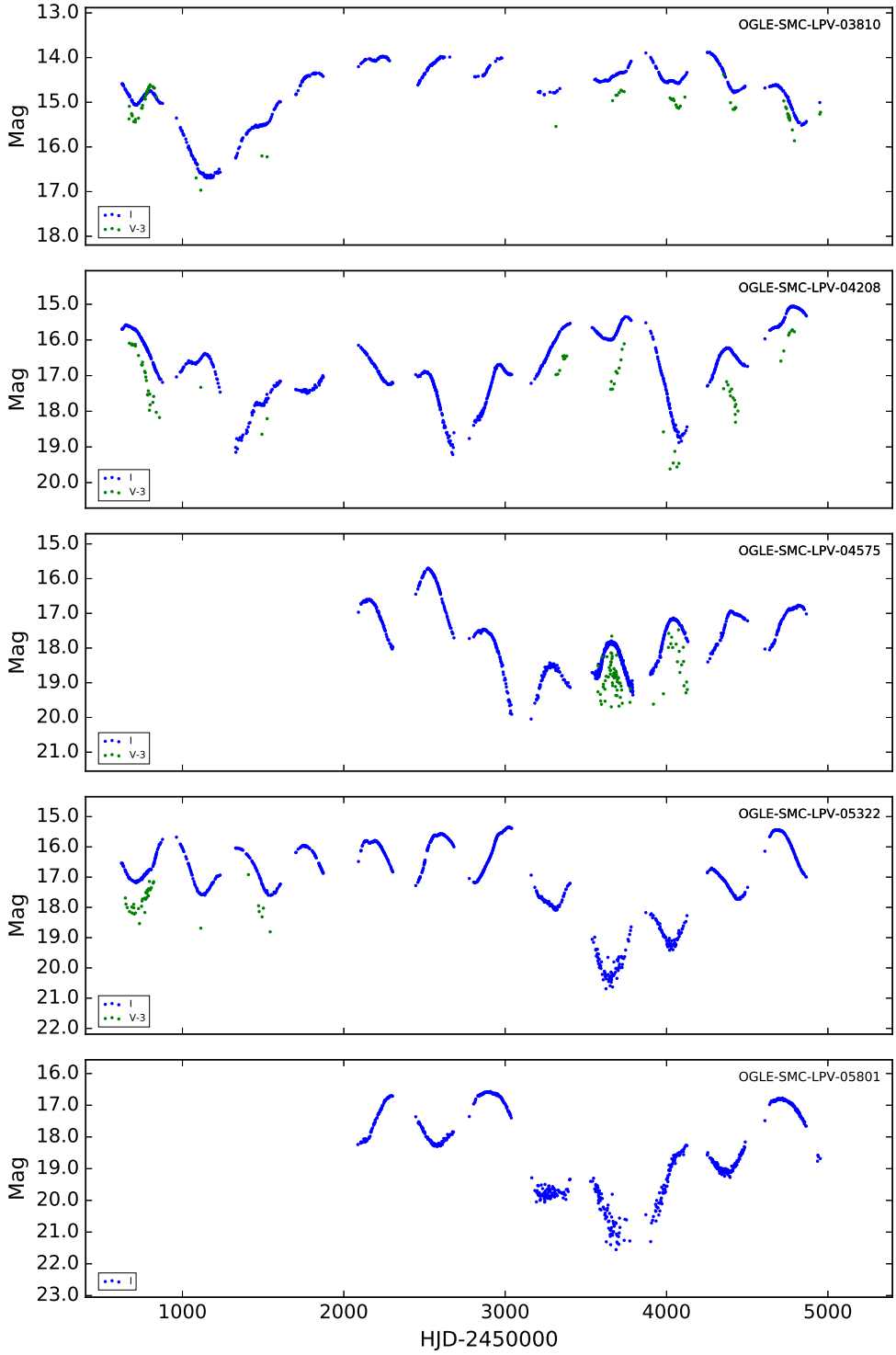


**Figure 4.** Light curves in $I$ (*blue*) and $V$ (*green*) of new DY Per candidates in the SMC.

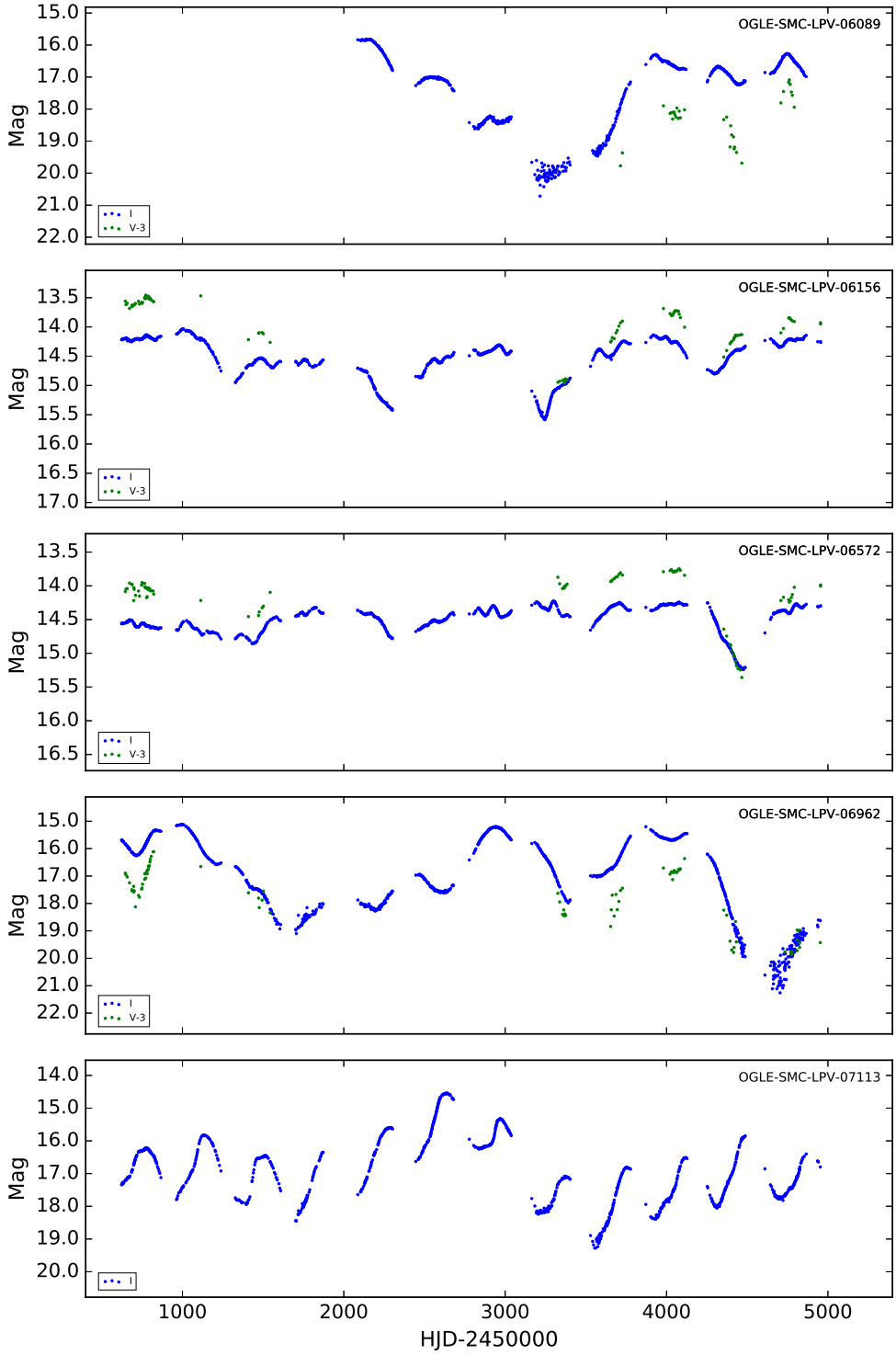


**Figure 5.** Light curves in $I$ (*blue*) and $V$ (*green*) of new DY Per candidates in the SMC.

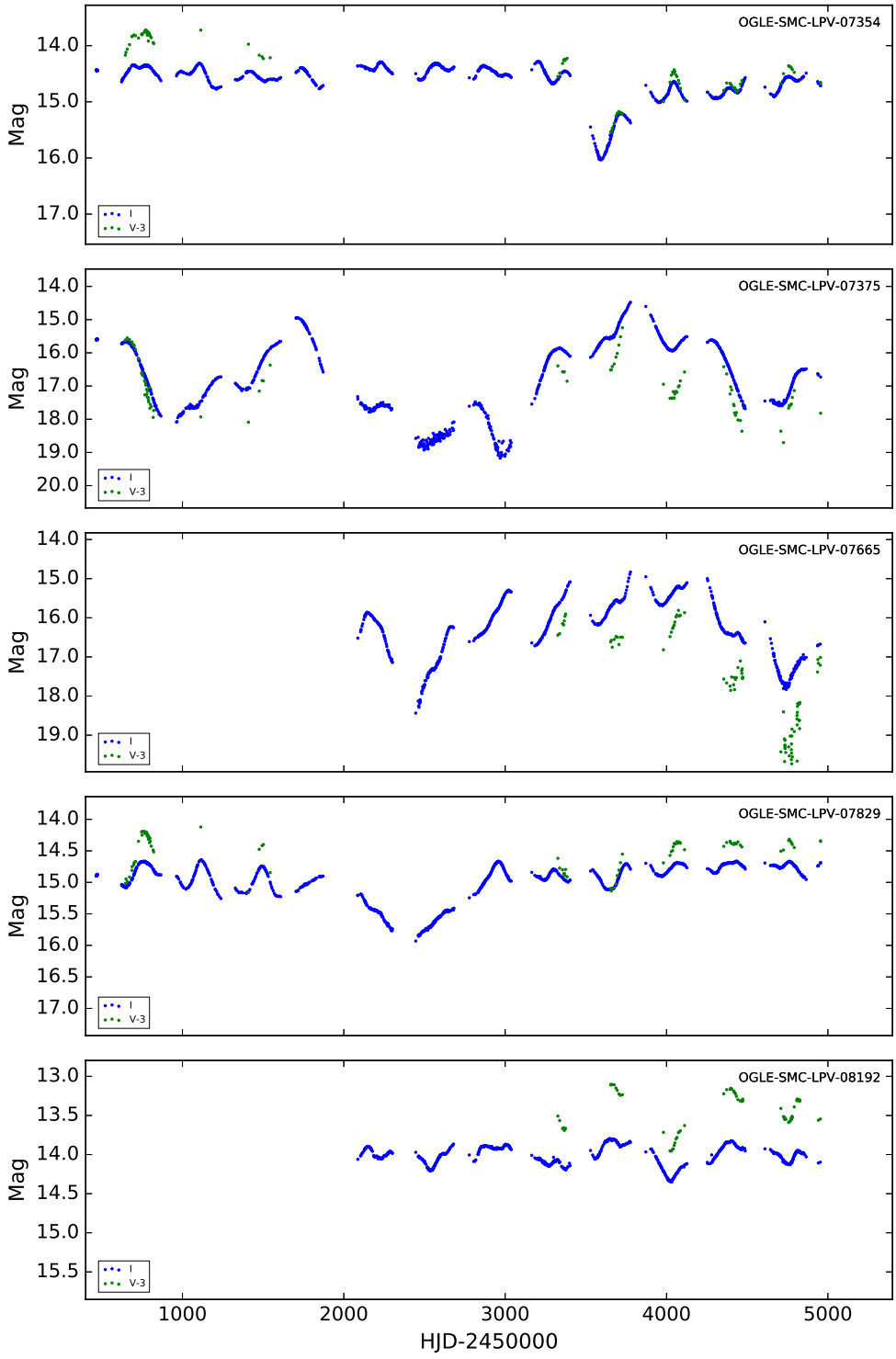


**Figure 6.** Light curves in $I$ (*blue*) and $V$ (*green*) of new DY Per candidates in the SMC.

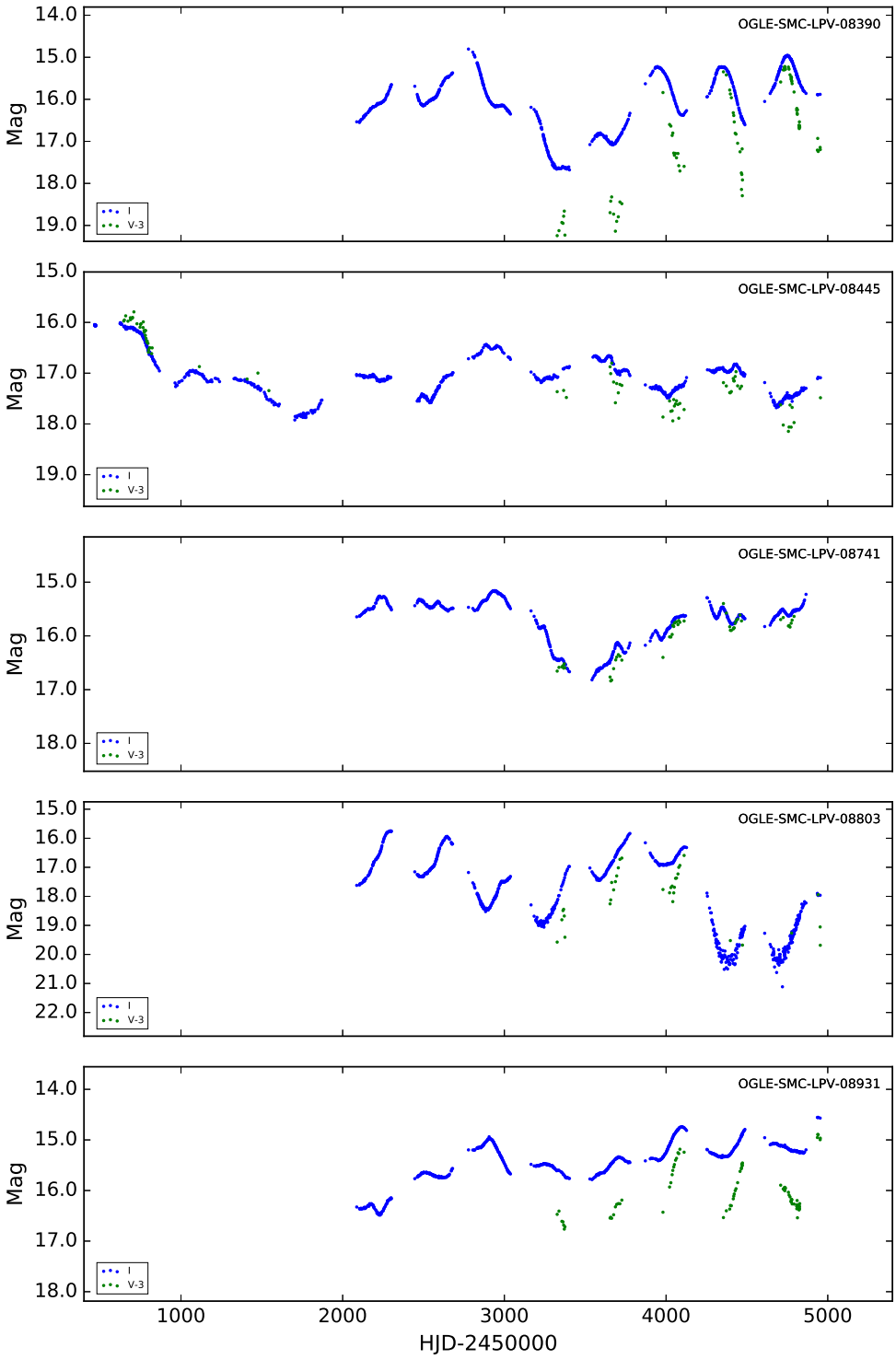


**Figure 7.** Light curves in $I$ (*blue*) and $V$ (*green*) of new DY Per candidates in the SMC.

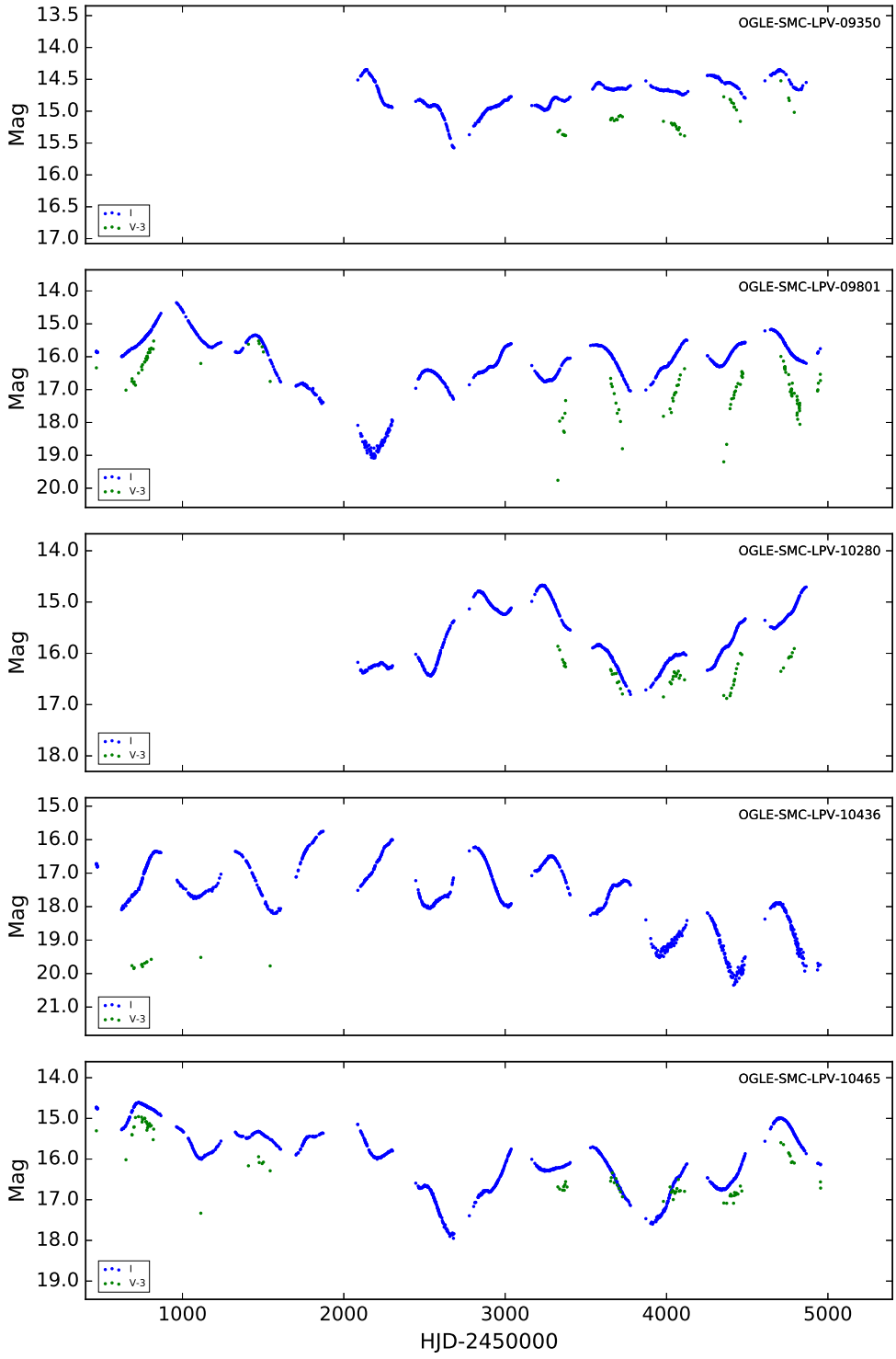


**Figure 8.** Light curves in $I$ (*blue*) and $V$ (*green*) of new DY Per candidates in the SMC.

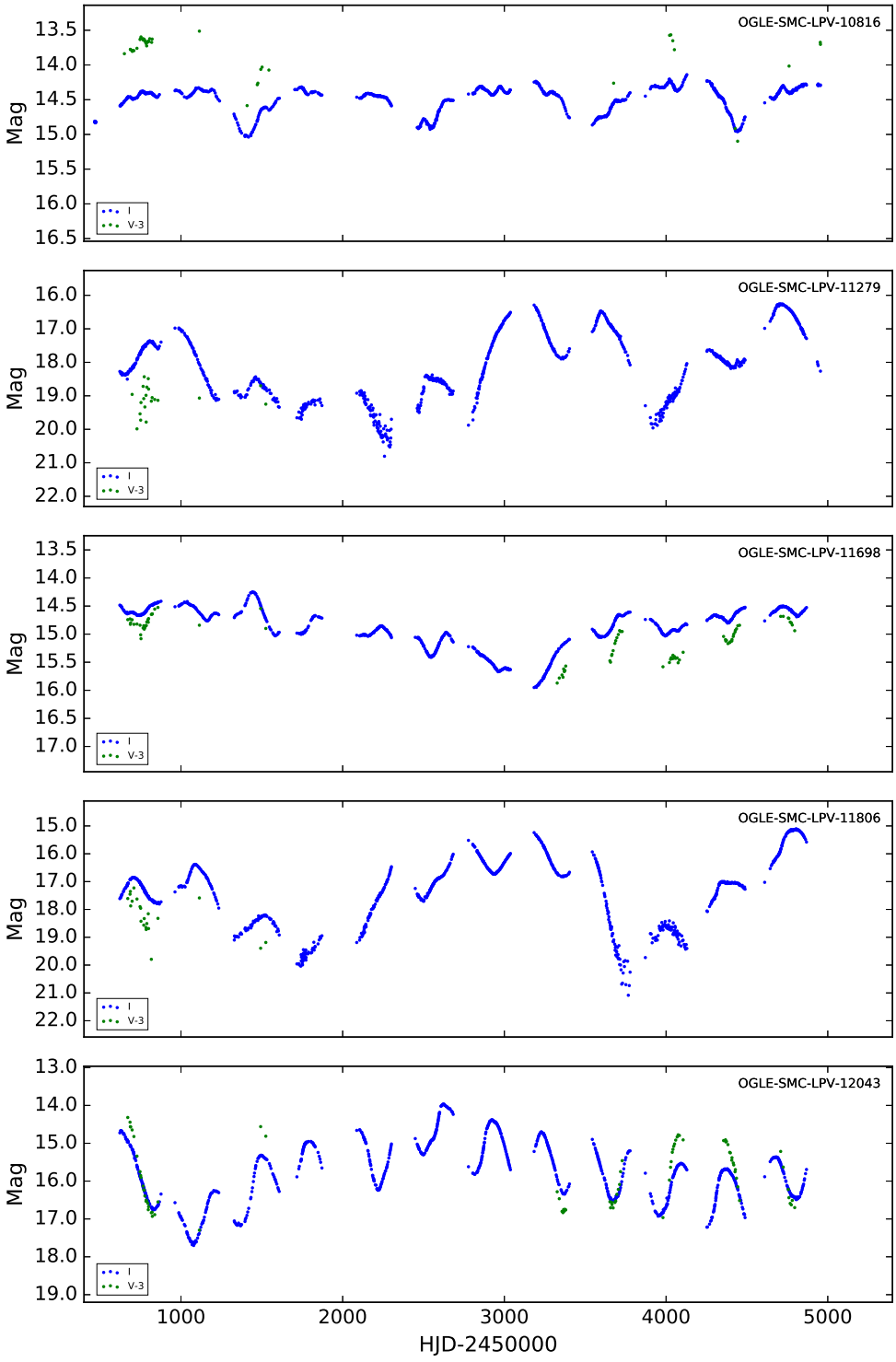


**Figure 9.** Light curves in $I$ (*blue*) and $V$ (*green*) of new DY Per candidates in the SMC.

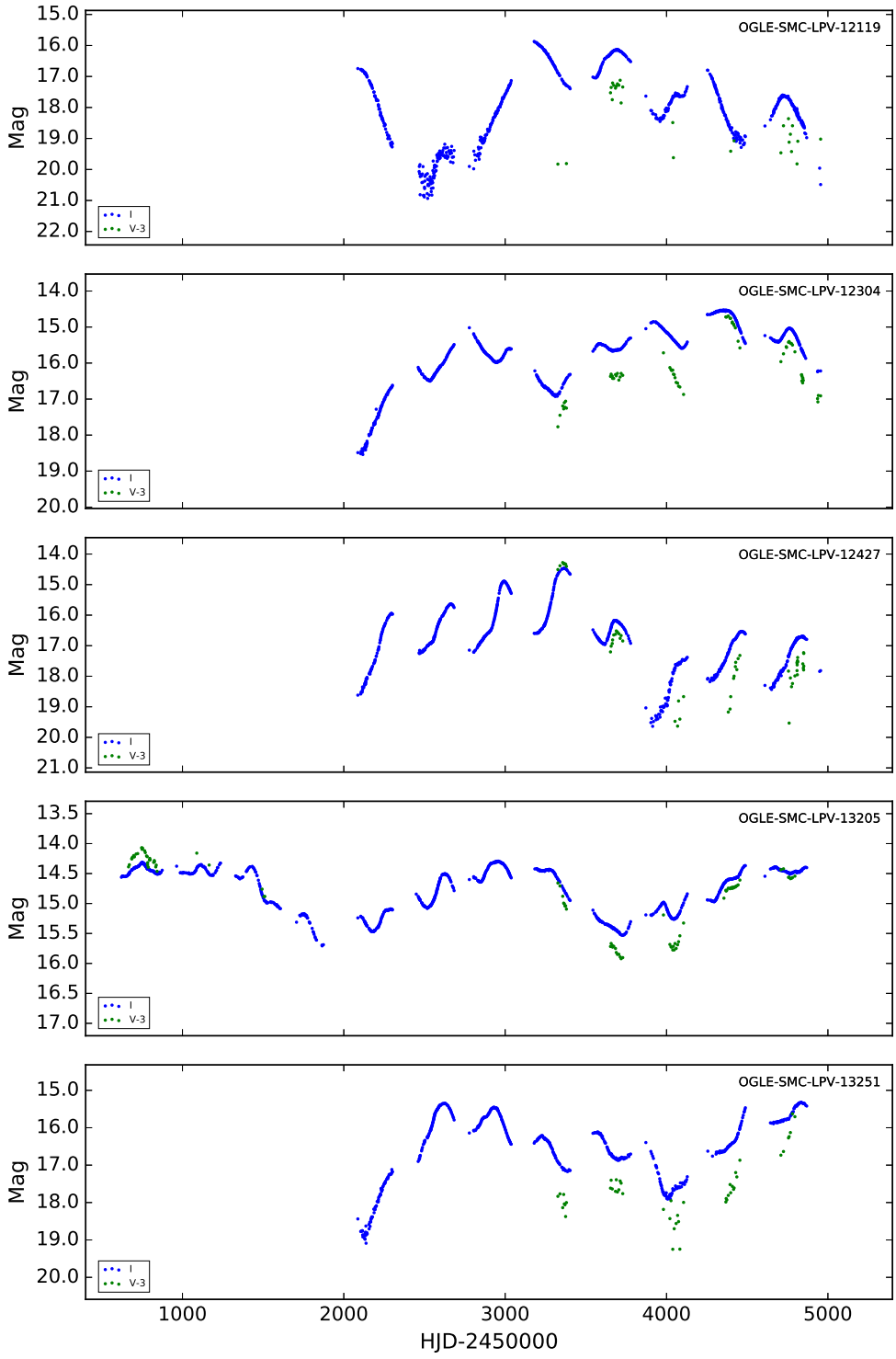


**Figure 10.** Light curves in $I$ (*blue*) and $V$ (*green*) of new DY Per candidates in the SMC.

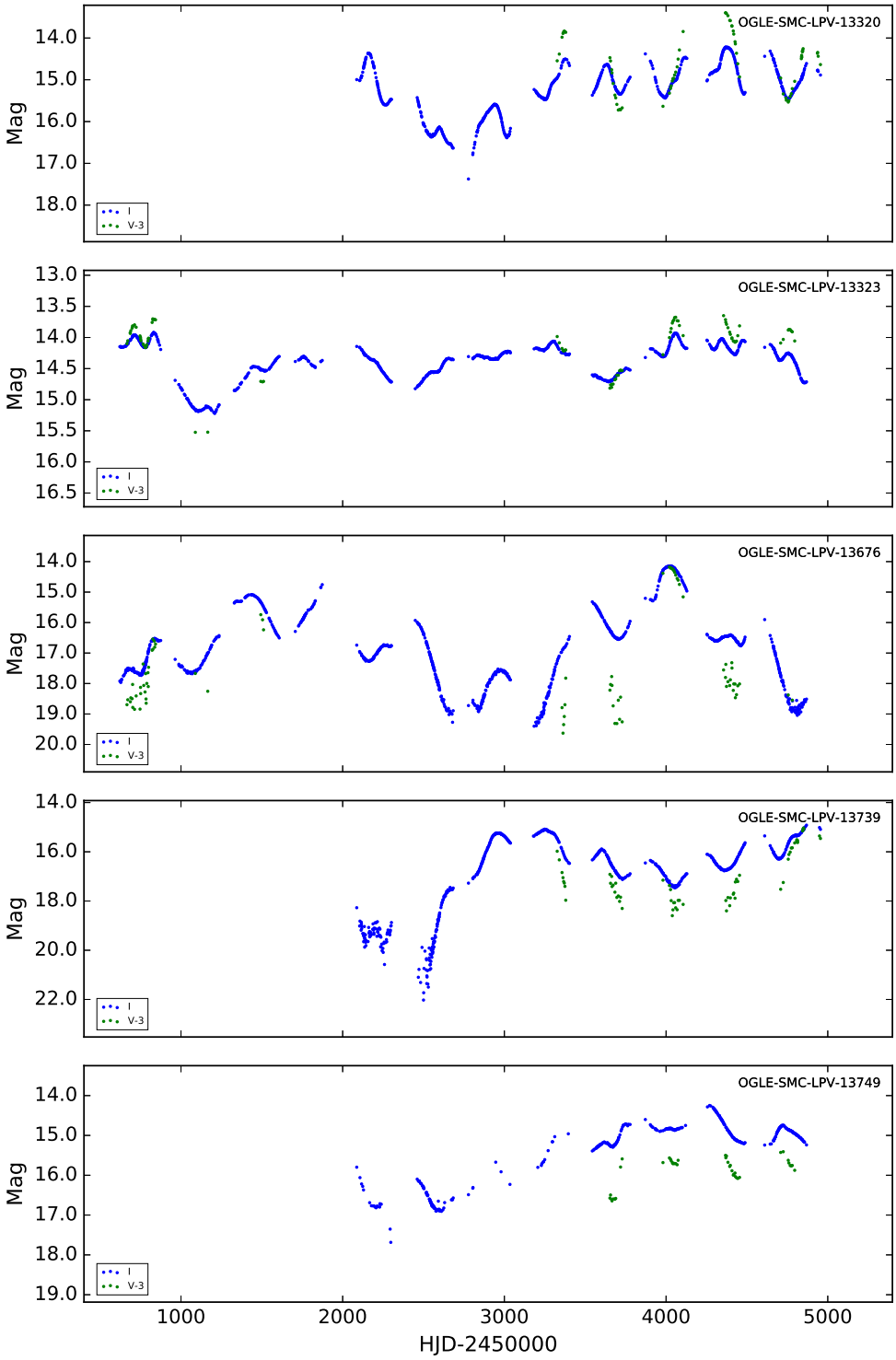


**Figure 11.** Light curves in $I$ (*blue*) and $V$ (*green*) of new DY Per candidates in the SMC.

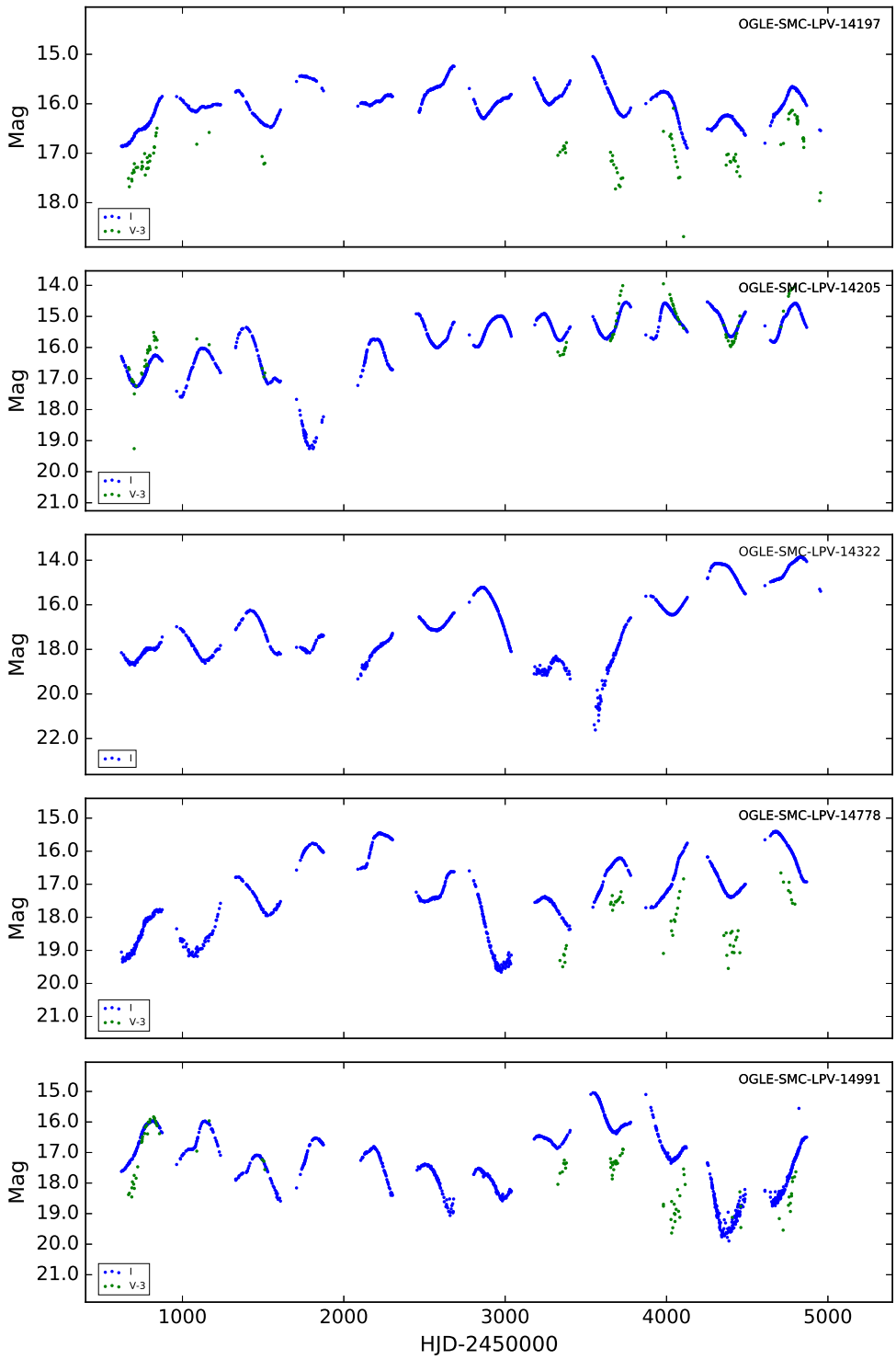


**Figure 12.** Light curves in $I$ (*blue*) and $V$ (*green*) of new DY Per candidates in the SMC.

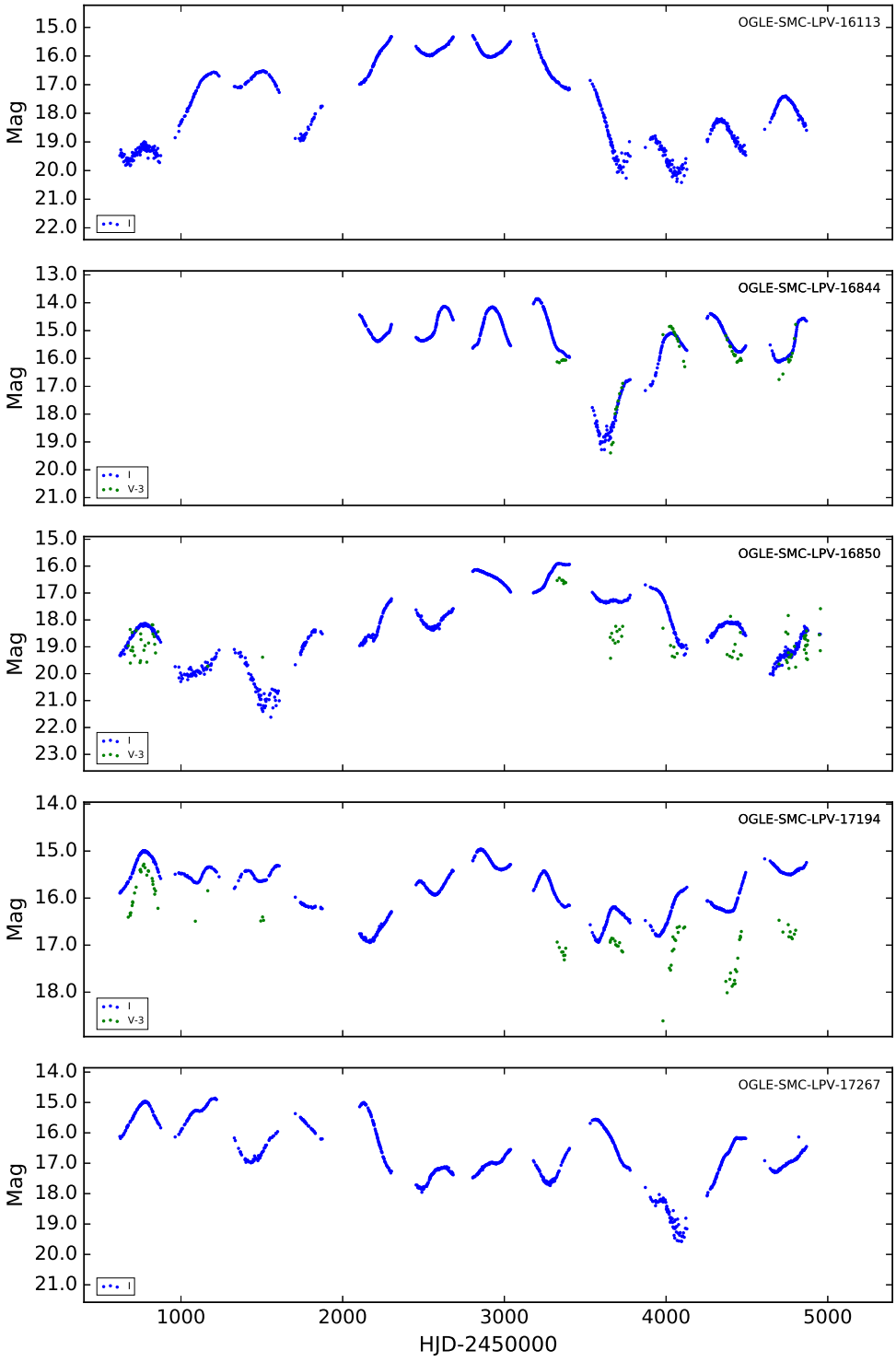


**Figure 13.** Light curves in $I$ (*blue*) and $V$ (*green*) of new DY Per candidates in the SMC.

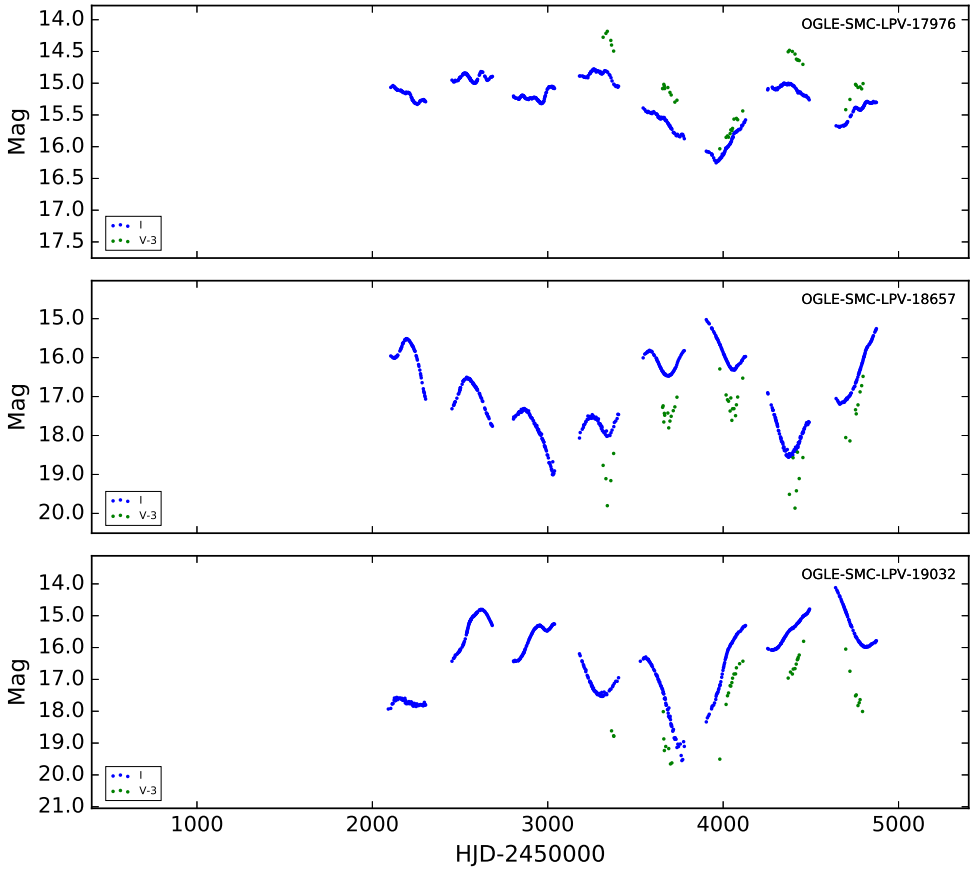


**Figure 14.** Light curves in $I$ (*blue*) and $V$ (*green*) of new DY Per candidates in the SMC.

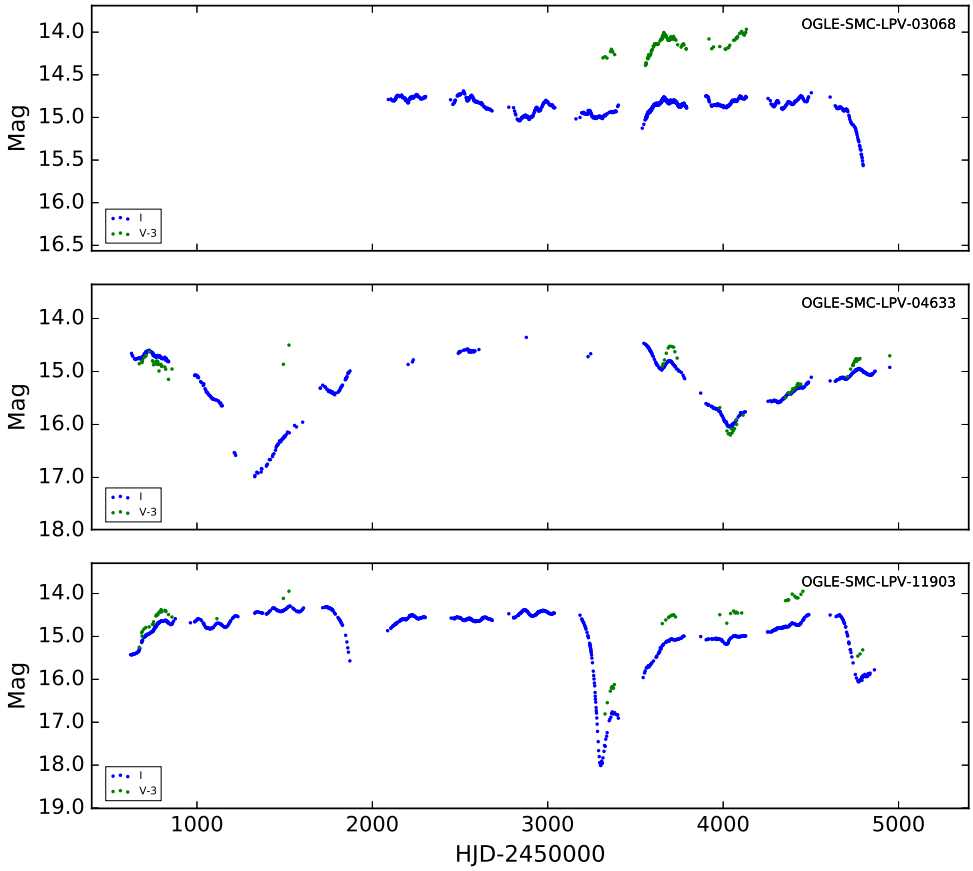


**Figure 15.** Light curves in $I$ (*blue*) and $V$ (*green*) of previously confirmed DY Per stars in the SMC (Tisserand et al. 2009), identified in this paper using OGLE data. Note the RCB-like light curve shape of OGLE-SMC-LPV-11903.

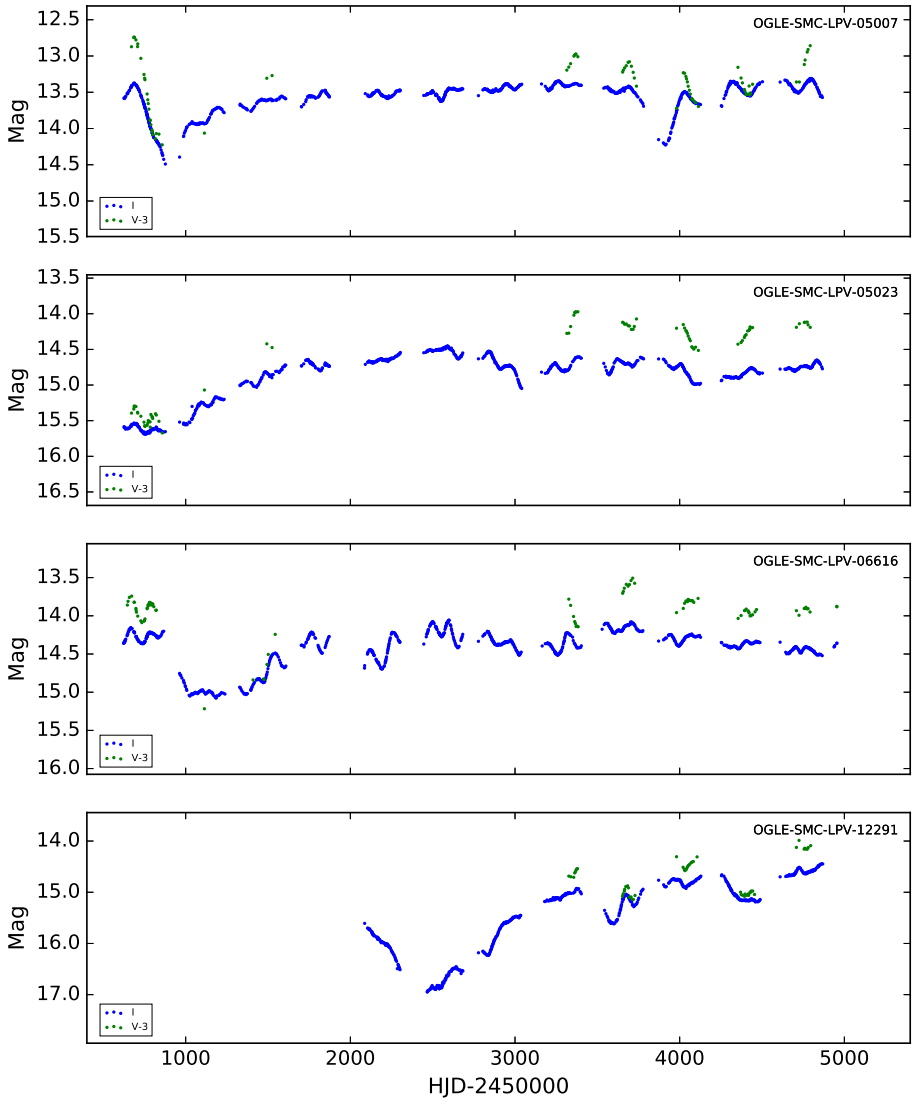


**Figure 16.** Light curves in $I$ (*blue*) and $V$ (*green*) of candidate DY Per stars in the SMC (Tisserand et al. 2009), identified in this paper using OGLE data. Note that we include in this plot the "borderline" DY Per-like star OGLE-SMC-LPV-05007 (see text for details).

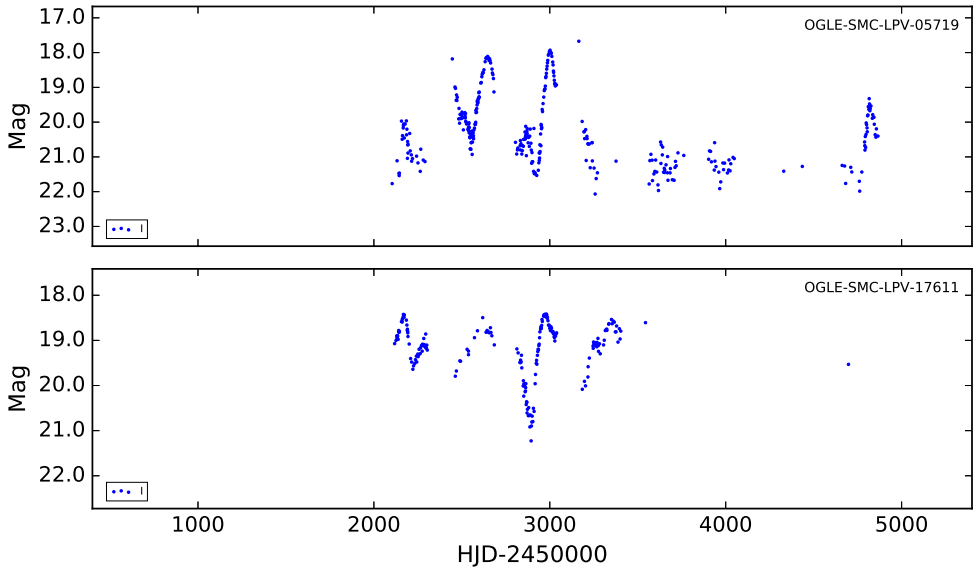


**Figure 17.** (*Upper panel*): light curve in $I$ (*blue*) of a known RCB candidate in the SMC (MSX-SMC-014; Kraemer et al. 2005), identified in this paper as OGLE-SMC-LPV-05719. (*Bottom panel*): our new RCB candidate OGLE-SMC-LPV-17611.